IEEE Photonics Journal
An IEEE Photonics Society Publication

Open Access

Highly Sensitive Optical Fiber Curvature and Acoustic Sensor Based on Thin Core Ultralong Period Fiber Grating

Volume 9, Number 2, April 2017

Wenjun Ni
Ping Lu
Xin Fu
Shun Wang
Yuan Sun
Deming Liu
Jiangshan Zhang

Graphical Abstract

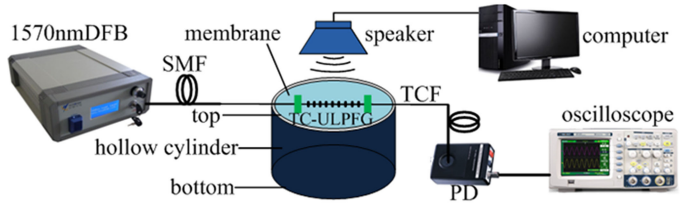

Schematic diagram of the experimental setup

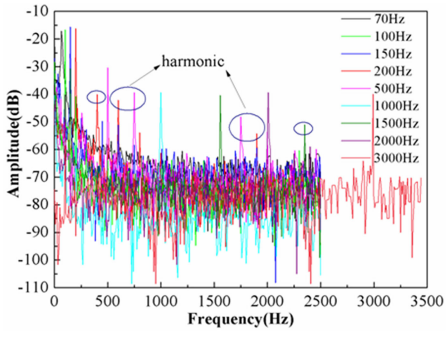

Frequency response range from 70Hz to 3kHz

DOI: 10.1109/JPHOT.2017.2665705
1943-0655 © 2017 IEEE

Highly Sensitive Optical Fiber Curvature and Acoustic Sensor Based on Thin Core Ultralong Period Fiber Grating

Wenjun Ni,[1] Ping Lu,[1] Xin Fu,[1] Shun Wang,[2] Yuan Sun,[1] Deming Liu,[1] and Jiangshan Zhang[3]

[1]School of Optical and Electronic Information, National Engineering Laboratory for Next Generation Internet Access System, Huazhong University of Science and Technology, Wuhan 430074, China
[2]Laboratory of Optical Information Technology, Wuhan Institution of Technology, Wuhan 430205, China
[3]School of Electronic Information and Communications, Huazhong University of Science and Technology, Wuhan 430074, China

DOI:10.1109/JPHOT.2017.2665705

Manuscript received November 19, 2016; revised February 1, 2017; accepted February 3, 2017. Date of publication February 8, 2017; date of current version February 27, 2017. This work was supported in part by the Natural Science Foundation of China under Grant 61275083 and Grant 61290315 and in part by the Fundamental Research Funds for the Central Universities under Grant HUST: 2014CG002.
Corresponding authors: P. Lu and D. Liu (e-mail: pluriver@mail.hust.edu.cn; dmliu@mail.hust.edu.cn).

Abstract: A novel fiber sensor for curvature and acoustic wave measurement, which is based on a thin core ultralong period fiber grating (TC-ULPFG), has been proposed and experimentally demonstrated. By tracking the power variation of different resonant wavelength caused by TC-ULPFG, high curvature sensitivity of 97.77 dB/m^{-1} is achieved, to best of our knowledge, which is the highest than other structures at the same measurement range. Thus, the desired curvature property of the TC-ULPFG is used for acoustic measurement. The polyethylene terephthalate film is selected as a transducer, on which TC-ULPFG is tightly pasted. The acoustic pressure sensitivity of 1.89 V/Pa is two orders higher than other structures based on the diaphragm transducer, and the noise-limited minimum detectable pressure is 1.94 mPa/Hz$^{1/2}$ at 200 Hz. In addition, the frequency fluctuations are nearly $\pm$0.4 dB from 70 to 200 Hz and $\pm$0.2 dB from 1 to 3 kHz. Therefore, the proposed optical fiber acoustic sensor has a flat frequency response at a relatively lower frequency. The TC-ULPFG shows many advantages, including high sensitivities of curvature, high acoustic pressure sensitivity, easy fabrication, simple structure, and low cost.

Index Terms: Thin core ultra-long period fiber grating (TC-ULPFG), optical fiber acoustic sensor (OFAS), flat frequency response.

1. Introduction

In recent years, the optical fiber acoustic sensor (OFAS) has been used in many important engineering applications, such as structural health monitoring [1], oil pipeline leakage detection [2], biomedical diagnosis [3], etc. OFASs are in general immune to electromagnetic interference (EMI), resistant to corrosion, and are highly sensitive. Therefore OFASs are superior to electronic and mechanical acoustic sensors in harsh environment. In order to realize combination of lower cost, compact size and high sensitivity, more and more optical fiber interferometric structures and optical fiber devices have been proposed and experimentally demonstrated. Some typical optical fiber

interferometric structures, including Mach-Zehnder (MZ) [4], Sagnac [5], Michelson [6], and Fabry-Perot (FP) interferometer [7], have been reported over the past decades, especially FPI based on thin films [8], [9]. However, most of the structures mentioned above have relatively large size, lower conversion efficiency with identical transducers and easily influenced by external environment variation. Consequently, more attention has been paid to simple optical fiber device.

It has been reported in the last five years that some optical fiber devices, such as optical fiber taper [10], [11], fiber coupler [12], [13], FP cavity based on pairs of fiber Bragg gratings (FBG-FP) [14], [15], and long period fiber grating (LPFG) [16] are widely used as sensor heads in OFAS. The transducers of these optical fiber devices are always based on thin films, thin metal plate, composite materials and water, etc. FBG-FP is relatively difficult to fabricate, moreover, the repetitive rate of its fabrication is not high. Optical fiber taper need to be inserted in other interferometric structure to introduced modal interference. Optical fiber coupler can measure the wideband response. However, the frequency response is always not flat. Compared with the above mentioned optical fiber devices, ultra-long period fiber grating (ULPFG) has significant superiority in the field of acoustic measurement, such as a single optical device without other cascaded interferometric structure and easy to fabricate. The most important advantage is that ULPFG possess high curvature sensitivity. Since acoustic measurement based on ULPFG is dynamic curvature detection in fact, ULPFG is a novel optical device and good candidate for dynamic parameters sensing. Recently, LPFG have been written in varies of special fiber, including thin core fiber (TCF) [17], photonic crystal fiber (PCF) [18], few mode fiber (FMF) [19], etc. To the best of our knowledge, no one has used TCF to inscribe ULPFG.

In this paper, a novel optical device TC-ULPFG with high curvature sensitivity is proposed and demonstrated. By tracking the power variation of different resonant wavelength, curvature sensitivity of 97.77 dB/m^{-1} is achieved, corresponding to the resonant wavelength of 1570 nm. Thus, TC-ULPFG is used for acoustic measurement, which has flat frequency response in two bands, 70 Hz $\sim$ 200 Hz and 1 kHz $\sim$ 3 kHz, respectively. Additionally, the minimum detectable pressure level is 1.94 mPa/$\sqrt{\text{Hz}}$ and the sensitivity of acoustic pressure is 1.89 V/Pa. The input acoustic signal is recovered in the method of intensity demodulation. The proposed sensor head shows many advantages including multi-parameters measurement, high sensitivity of curvature, easy fabrication, simple structure, and low cost.

2. Static Properties of the Sensor Head

The TC-ULPFG is inscribed by the focused CO_2 laser pulse (SYNRAD, 48-series) on one side of TCF using point-by-point method, and the experiment setup of fabrication process has been published recently [20]. It is obvious that the differences between TC-ULPFG and thin core long period fiber grating (TC-LPFG) are number of periods and grating pitch. TC-ULPFG has an ultra-long grating pitch, which is twice the published TC-LPFG. The number of periods, grating pitch and the diameter of TCF (YOEC, 15-80-U16, 80 μm) are 30, 1 mm, and 80 μm, respectively. The transmission spectrum of TC-ULPFG is shown in Fig. 1, and the inset is schematic diagram of the sensor head. The proposed structure is composed of five sections named Input-SMF(ISMF), Input-TCF(ITCF), TC-ULPFG, Output-TCF(OTCF) and Output-SMF(OSMF), which can be fabricated only by the fusion splicer (Fujikura, FSM-60S). The ITCF and OTCF are cut off by 15 cm with fiber cleaver (Fujikura, CT-38) to avoid the influence of modal interference [17], [20]. Because the length of TCF is relatively long, nearly all of the cladding modes excited by the mode field mismatch or TC-ULPFG will undergo entirely loss in the TCF. The transmission of all the fiber modes will experience with the following two process. Firstly, cladding modes will be excited in ITCF at the first splicing point due to the mode field mismatch between ISMF and ITCF, and will undergo completely loss in ITCF because of the long length of ITCF [17]. Secondly, cladding modes will be excited again at the grating region due to the mode coupling between core and cladding modes in TC-ULPFG [21], and will disappear in OTCF for the same reason. Since the coupling between the core and cladding modes is wavelength dependent, several resonant dips will be introduced in the transmission spectrum. It can be seen from the Fig. 1 that there are four dominant dips generated

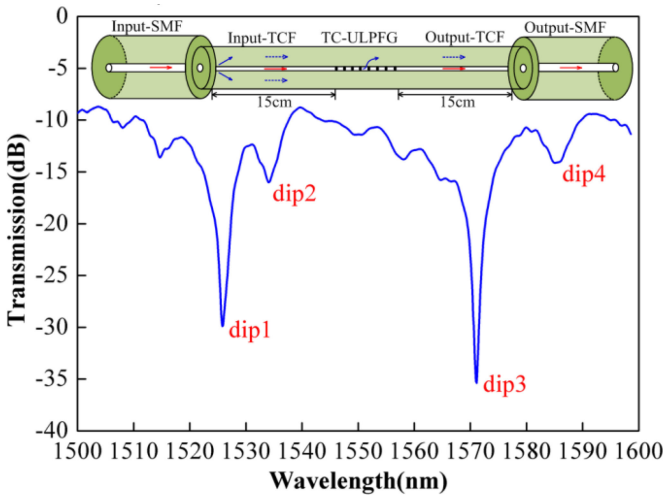

Fig. 1. Schematic diagram of the sensor head and transmission spectrum.

by TC-ULPFG which are called dip1, dip2, dip3, and dip4 from left to right, respectively. The location of dip3 is close to 1570 nm, and the extinction ratio is nearly 25 dB. Moreover, the 3 dB bandwidth of dip3 is 3.5 nm, which is narrower than any reported common LPFG. When the number of scanning circles is increasing, the 3 dB bandwidth is generally decreasing and the extinction ratio is generally increasing. The 3 dB measurement can be detected by the optical spectrum analyzer (OSA) or the software of originlab. Taking these advantages of TC-ULPFG into consideration, the resonant wavelength of TC-ULPFG can be well used for the intensity demodulation.

Curvature is a static parameter, so the measurement process is relatively simple. Only an amplified spontaneous emission (ASE) light source, optical spectrum analyzer (OSA, Yokogawa AQ6370c) and 2-D translation stages (Zolix) are needed. It is worth noting that the sensor head should keep straight line without external axial tension. The curvature is increased by reducing the distance between two translation stages. As shown in Fig. 2(a), the intensity of dip1 and dip3 are increasing with the curvature increasing from 0.4243 m^{-1} to 0.5475 m^{-1}. Furthermore, another two dips are gradually disappearing. Thus, dip1 and dip3 are selected to detect the curvature variation. The extinction ratio of dip1 and dip3 decrease with the increased curvature due to part of the cladding modes leaking out. As shown in Fig. 2(a), the power of the dip2 and dip4 are generally decreasing. As we all know, there are sidelobes in TC-ULPFG. Thus, the two different dips corresponding to the two cladding modes have mode competition. If the power of the main dip is decreasing, the power of the sidelobes of the TC-ULPFG will increase. The following figure shows that dip1 and dip3 are the dominant resonant wavelength. Therefore, the trend of dip1 and dip3 are different from that of dip2 and dip4. When curvature increases from 0.4243 m^{-1} to 0.5475 m^{-1}, linear intensity variations of dip1 and dip3 with the sensitivities of 69.43 dB/m^{-1} and 97.77 dB/ m^{-1} are achieved, as shown in Fig. 2(b). The blue line of the circle point is the linear fit of dip1 and the red line of the square point is the linear fit of dip3. Different sensitivities of dip1 and dip3 are caused by the different order of cladding modes and different diffraction order. From Fig. 2(b), it can be seen that there are nearly no wavelength shift. Only intensity variation of dip1 and dip3 can be observed. Therefore, high curvature sensitivities based on intensity demodulation can be obtained by the proposed TC-ULPFG. As is known to all that the acoustic signal detection can be converted to the dynamic curvature measurement. Given the above discussion, an OFAS can be realized based on TC-ULPFG because of its high curvature sensitivities.

3. Theoretical Analysis of Acoustic Signal Demodulation

For acoustic sensing, good transducer is a vital device in acoustic signal measurement processing. Membrane is a very common transducer mentioned by the last report. The PET film is selected as

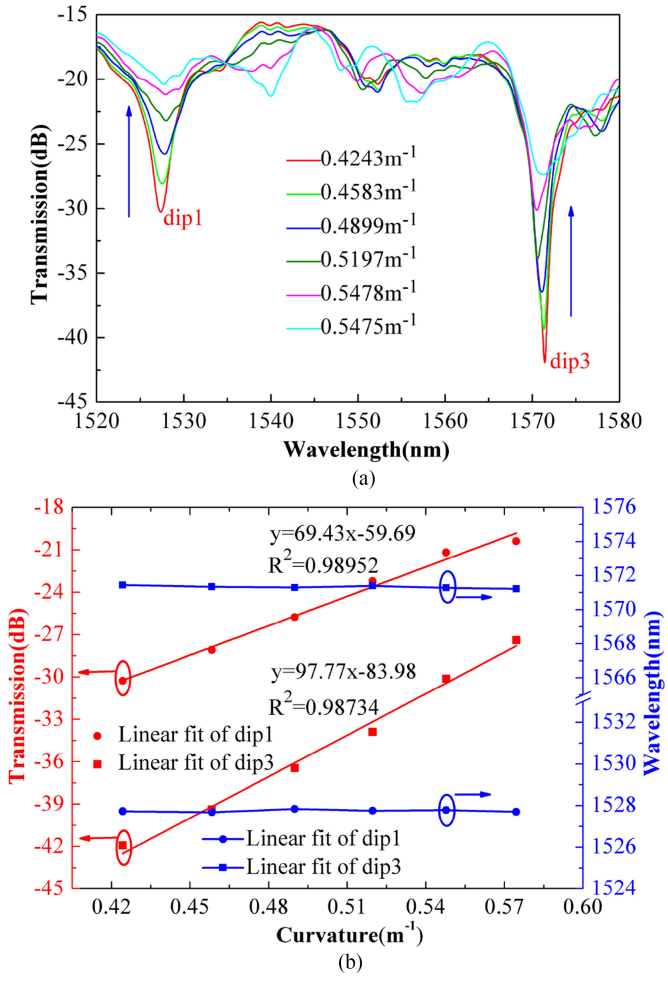

Fig. 2. (a) Transmission spectrum with curvature increasing from 0.4243 m^{-1} to 0.5475 m^{-1}. (b) Linear fit of dip1 and dip3 with sensitivities of 69.43 dB/m^{-1} and 97.77 dB/m^{-1}, respectively.

the following acoustic sensing, as shown in the inset of Fig. 3. The acoustic conversion setup is based on a circular PET film where a TC-ULPFG is adhered on the central axis. It should be noticed that the TC-ULPFG has a tiny pre-bending to avoid frequency doubling phenomenon [16]. When the acoustic wave is applied on the membrane, the acoustic signal is converted to the vibration. Consequently, the membrane will deform due to its vibration. The film deformation equation can be described as [22]

$$S_{def} = \frac{\Delta L}{\Delta P} = \frac{3(1-\mu^2)r^4}{16Eh^3}. \tag{1}$$

In order to study the characteristics of the frequency response, the PET film can be regarded as a thin plate. Similarly, the resonant frequency f_{res} of the diaphragm can be expressed as [23]

$$f_{res} = \frac{10.21h}{2\pi r^2}\sqrt{\frac{E}{12\rho(1-\mu^2)}}. \tag{2}$$

In the above equations, r, h, μ, ρ, and E are the radius, thickness, Poisson ratio, mass density and Young's modulus of the PET film, respectively. The parameters of PET film are as follows: $\mu = 0.39$, $\rho = 1.38 \times 10^3$ kg/m^2, and $E = 2.5$ GPa. As shown in Fig. 3, the resonant frequency is in

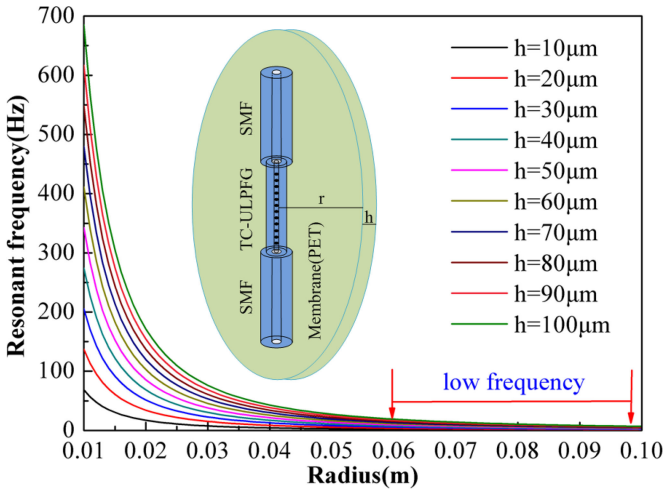

Fig. 3. Relationship between resonant frequency and radius with different thickness of PET film.

negative correlation with the film thickness, and the lower resonant frequency is mainly generated with the radius ranging from 0.06 m to 0.1 m. In Section 2, the length of the TC-ULPFG is 3 cm. The TC-ULPFG must be pasted on the PET film. In our work, the adhesive tape is applied to fix the TC-ULPFG on the middle of the membrane. Therefore, the diameter of the membrane should have an enough length to fix the device. If the diameter of the membrane is too short, the grating region is easy to be broken. Thus, the diameter of the PET film is about three times longer than the TC-ULPFG. When the diameter of the membrane is a certain value, the resonant frequency is increasing with the thickness of the membrane increasing. Therefore, the film thickness is positive correlation of the resonant frequency. According to the (2), it also can be seen that the relationship between resonant frequency and the film thickness is positive correlation. In order to detect lower frequency, Radius is better to be selected as the average value which is 0.08 m. It can be seen from Fig. 3 that the lower resonant frequency bands are close to a straight line no matter how to change the thickness of PET film. Thus, the thickness of PET film is also selected as the mid-value which is 50 μm. According to the (1), the static pressure sensitivity induced by the membrane deformation is 208 cm/Pa. In addition, the resonant frequency of the PET film is calculated to be 5.36 Hz from (2). The two parameters obtained by the above analysis are very important in acoustic measurement fields.

The acoustic signal measurement based on TC-ULPFG is dynamic curvature detection in fact. As shown in Fig. 2(b), there are nearly no wavelength shift of dip1 and dip3, but only intensity variation while measuring the static curvature [25]. The 1570 nm Distributed Feedback Laser (DFB, long-term stability: $\leq \pm 0.02$ dB) is used as the laser source since the resonant wavelength of dip3 is 1570 nm. The schematic diagram of the intensity demodulation is exhibited in Fig. 4. When the input acoustic signal is applied on the PET film, the laser intensity will vary periodically. Then the output signal will be a time domain waveform after photovoltaic conversion. Therefore, the acoustic signal can be real time demodulated by detecting the intensity of output optical signal.

4. Experimental Results and Discussions

The experimental setup of acoustic measurement is shown in Fig. 5, including 1570 nm DFB laser, acoustic source, membrane, TC-ULPFG, photoelectric detector (PD), and oscilloscope, etc. The membrane is closely pasted on the hollow cylinder, which the bottom is closed and the top is open. The placement of the membrane is shown in the following schematic diagram. Additionally, the membrane is parallel to the bottom and the surface of the membrane must keep flat. TC-ULPFG fixed by adhesive is pasted in the middle of the membrane, and the acoustic source is placed in

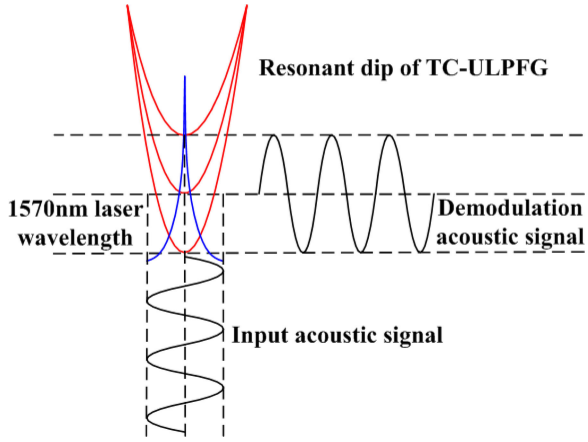

Fig. 4. Principle of the intensity demodulation.

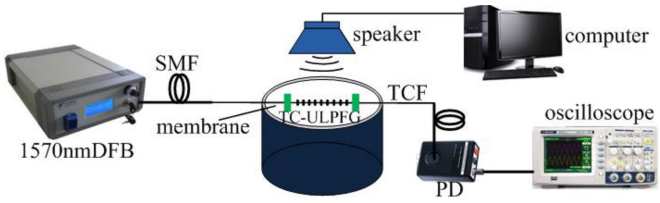

Fig. 5. Schematic diagram of the experimental setup.

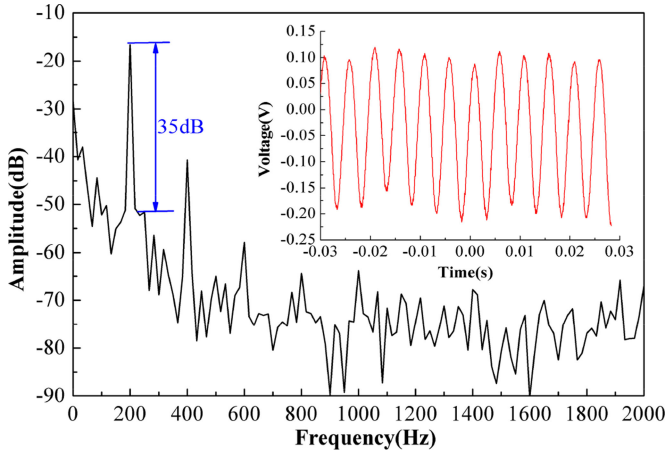

Fig. 6. Frequency spectrum response and time domain waveform at 200 Hz.

the above of the membrane. The distance between acoustic source and membrane is controlled to nearly 10 cm to sustain a consistent response of the membrane. The acoustic source is controlled by the computer to regulate acoustic frequency. The light intensity variation is detected by the PD, and displayed on the oscilloscope.

In view of dynamic parameter sensing, TC-ULPFG has a dominant advantage of high curvature sensitivity. A single frequency acoustic signal is given by the computer, and it is recovered by the demodulation method mentioned before. The inset of Fig. 6 shows the time domain waveform at the frequency of 200 Hz. The frequency spectrum response of 200 Hz is obtained by taking Fast Fourier Transform (FFT), which is shown in Fig. 6. It is observed that there are odd harmonics and even harmonics in the frequency spectrum simultaneously. The existence of the harmonics is

TABLE 1
COMPARISON RESULT OF DIFFERENT STRUCTURE FOR CURVATURE AND ACOUSTIC MEASUREMENT

Structure	Curvature sensitivity	Acoustic pressure sensitivity	Minimum detectable pressure	Ref.
Inline MZ interferometer	70.03 dB/m^{-1}			[25]
Diaphragm-based LPFG	13.5 nm/m^{-1}	60.52 mV/Pa	1.42 mPa	[16]
Diaphragm-based FP		13.15 mV/Pa	75 μPa/$\sqrt{\text{Hz}}$	[23]
Proposed	97.77 dB/m^{-1}	1.89 V/Pa	1.94 mPa/$\sqrt{\text{Hz}}$	ours

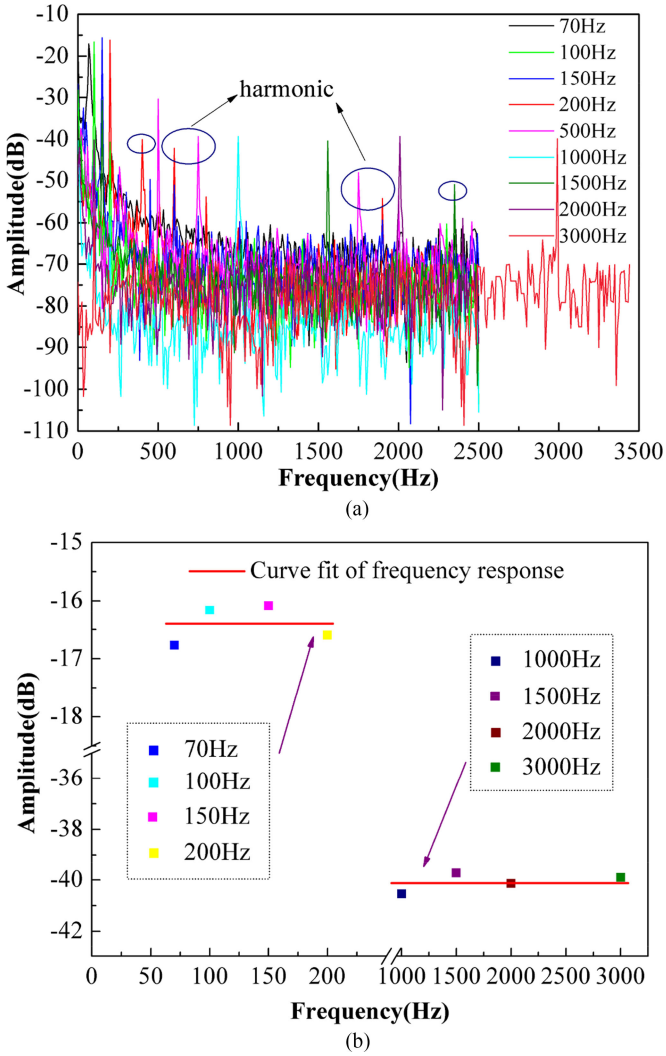

Fig. 7. (a) Frequency response range from 70 Hz to 3 kHz. (b) Frequency fluctuation from 70 Hz to 200 Hz and from 1 kHz to 3 kHz.

caused by the indoor reflection of the acoustic wave. The signal-to-noise (SNR) at 200 Hz is 35 dB. The power frequency of 50 Hz can be nearly neglected because it is close to the noise level. The 3 dB bandwidth at 200 Hz is 2.12 Hz, and the acoustic pressure applied on the PET film is 78 dB,

corresponding to a noise-limited minimum detectable pressure level of 1.94 mPa/$\sqrt{\text{Hz}}$. Besides, the sensitivity of acoustic pressure is 1.89 V/Pa, which is two orders higher than the previously reported sensor of diaphragm-based FP cavity, etc. The comparison result is listed in Table 1.

The proposed TC-ULPFG has a very high acoustic pressure sensitivity which is mentioned above. Furthermore, in order to investigate the characteristics of the frequency response, a wide frequency test is carried out in a continuous frequency spectrum. In the acoustic wave experiment, the frequency from 70 Hz to 3 kHz can be measured, as shown in Fig. 7(a). The experiment result exhibits that the sensor head or the transducer is sensitive to the relatively lower frequency, which is consistent with the simulation result in Fig. 3. The proposed structure can measure infrasound and low frequency acoustic signal according to the theoretical analysis in Section 3. Therefore, the strong response appears when the frequency is lower than 200 Hz. However, the response to other frequencies are generally decreasing with the acoustic frequency increasing since the resonant frequency of the selected PET film is 5.36 Hz. When the acoustic frequency is higher than 1 kHz, the frequency response approximately trends to be stable because relatively higher frequency is far away from the resonant frequency. In Fig. 7(b), the frequency fluctuations are nearly $\pm$0.4 dB from 70 Hz to 200 Hz and $\pm$0.2 dB from 1 kHz to 3 kHz, respectively. The red line of the square point is the curve fit of the frequency response from 70 Hz to 3000 Hz. As a consequence, the proposed TC-ULPFG has a flat frequency response when the measurand is relatively close or far away from the resonant frequency.

5. Conclusion

In summary, we propose a novel fiber sensor based on TC-ULPFG for curvature and acoustic measurement. TC-ULPFG is fabricated by the focused CO_2 laser pulse on one side of TCF by the method of point-by-point. The high curvature sensitivities of 69.43 dB/m^{-1} and 97.77 dB/m^{-1} are achieved by tracking the power variation of dip1 and dip3, respectively. TC-ULPFG has a better curvature property, which is highest than other structures at the same measurement range. Additionally, this special optic device is used for acoustic measurement. The PET film is selected as the transducer, the thickness and radius of which are 50 μm and 8 cm, respectively. According to the theoretical analysis, membrane deformation and the resonant frequency are 208 cm/Pa and 5.36 Hz. In acoustic experiment, the acoustic pressure sensitivity is 1.89 V/Pa which is two orders higher than other structures of diaphragm-based transducer. The noise-limited minimum detectable pressure level is 1.94 mPa/ Hz$^{1/2}$ at 200 Hz. Moreover, the frequency fluctuations are nearly $\pm$0.4 dB from 70 Hz to 200 Hz and $\pm$0.2 dB from 1 kHz to 3 kHz, respectively. As a consequence, the proposed OFAS has a flat frequency response in relatively lower frequency. The TC-ULPFG shows many advantages including high sensitivities of curvature, high acoustic pressure sensitivity, easy fabrication, simple structure and low cost. Therefore, the proposed sensor may have a great potential in the fields of engineering system.

References

[1] C. Hu, Z. Yu, and A. Wang, "An all fiber-optic multi-parameter structure health monitoring system," *Opt. Exp.*, vol. 24, no. 18, pp. 20287–20296, 2016.
[2] Z. Wang and Z. Liu, "Design and experiment of data acquisition system of submerged buoy," *Ocean Technol.*, vol. 32, no. 4, pp. 6–10, 2013.
[3] H. Tazawa, T. Kanie, and M. Katayama, "Fiber-optic coupler based refractive index sensor and its application to biosensing," *Appl. Phys. Lett.*, vol. 91, no. 11, 2007, Art.ID. 113901.
[4] D. Pawar, C. N. Rao, R. K. Choubey, and S. N. Kale, "Mach-Zehnder interferometric photonic crystal fiber for low acoustic frequency detections," *Appl. Phys. Lett.*, vol. 108, no. 4, 2016, Art.ID. 041912.
[5] J. Kang, X. Dong, Y. Zhu, S. Jin, and S. Zhuang, "A fiber strain and vibration sensor based on high birefringence polarization maintaining fibers," *Opt. Commun.*, vol. 322, pp. 105–108, 2014.
[6] L. Liu *et al.*, "Fiber-optic michelson interferometric acoustic sensor based on a PP/PET diaphragm," *IEEE Sens. J.*, vol. 16, no. 9, pp. 3054–3058, May 2016.
[7] F. Xu, J. Shi, K. Gong, H. Li, R. Hui, and B. Yu, "Fiber-optic acoustic pressure sensor based on large-area nanolayer silver diaghragm," *Opt. Lett.*, vol. 39, no. 10, pp. 2838–2840, 2014.

[8] L. Liu *et al.*, "UV adhesive diaphragm-based FPI sensor for very-low-frequency acoustic sensing," *IEEE Photon. J.*, vol. 8, no. 1, Feb. 2016, Art. ID. 6800709.
[9] J. Ma, Y. Yu, and W. Jin, "Demodulation of diaphragm based acoustic sensor using Sagnac interferometer with stable phase bias," *Opt. Exp.*, vol. 23, no. 22, pp. 29268–29278, 2015.
[10] B. Xu *et al.*, "Acoustic vibration sensor based on nonadiabatic tapered fibers," *Opt. Lett.*, vol. 37, no. 22, pp. 4768–4770, 2012.
[11] Y. Li, X. Wang, and X. Bao, "Sensitive acoustic vibration sensor using single-mode fiber tapers," *Appl. Opt.*, vol. 50, no. 13, pp. 1873–1878, 2011.
[12] F. Li, Y. Liu, L. Wang, and Z. Zhao, "Investigation on the response of fused taper couplers to ultrasonic wave," *Appl. Opt.*, vol. 54, no. 23, pp. 6986–6993, 2015.
[13] S. Wang, P. Lu, L. Zhang, D. Liu, and J. Zhang, "Optical fiber acoustic sensor based on nonstandard fused coupler and aluminum foil," *IEEE Sens. J.*, vol. 14, no. 7, pp. 2293–2298, Jul. 2014.
[14] C. Lyu, Y. Liu, and C. Wu, "Wide bandwidth dual-frequency ultrasound measurements based on fiber laser sensing technology," *Appl. Opt.*, vol. 55, no. 19, pp. 5057–5062, 2016.
[15] X. Wang, L. Jin, J. Li, Y. Ran, and B. Guan, "Microfiber interferometric acoustic transducers," *Opt. Exp.*, vol. 22, no. 7, pp. 8126–8135, 2014.
[16] J. O. Gaudron, F. Surre, T. Sun, and K. T. V. Grattan, "LPG-based optical fibre sensor for acoustic wave detection," *Sens. Actuators A Phys.*, vol. 173, no. 1, pp. 97–101, 2012.
[17] C. Fu *et al.*, "Thin-core-fiber-based long-period fiber grating for high-sensitivity refractive index measurement," *IEEE Photon. J.*, vol. 7, no. 6, Dec. 2015, Art. ID. 7103208.
[18] F. Tian, J. Kanka, B. Zou, K. S. Chiang, and H. Du, "Long-period gratings inscribed in photonic crystal fiber by symmetric CO2 laser irradiation," *Opt. Exp.*, vol. 21, no. 11, pp. 13208–13218, 2013.
[19] B. Wang *et al.*, "CO2-laser-induced long period fiber gratings in few mode fibers," *IEEE Photon. Technol. Lett.*, vol. 27, no. 2, pp. 145–148, Jan. 2015.
[20] W. Ni *et al.*, "Bending direction detective fiber sensor for dual-parameter sensing based on an asymmetrical thin-core long-period fiber grating," *IEEE Photon. J.*, vol. 8, no. 4, Aug. 2016, Art. ID. 6803811.
[21] E. M. Dianov, S. A. Vasiliev, A. S. Kurkov, O. I. Medvedkov, and V. N. Protopopov, "IN-FTOER Mach-Zehnder interferometer based on a pair of long-period GratINGS," in *Proc. 22nd Eur. Conf. Opt. Commun.*, 1996, pp. 65–68.
[22] S. Wang *et al.*, "An infrasound sensor based on extrinsic fiber-optic Fabry–Perot interferometer structure," *IEEE Photon. Technol. Lett.*, vol. 28, no. 11, pp. 1264–1267, Jun. 2016.
[23] J. Ma, H. Xuan, H. L. Ho, W. Jin, Y. Yang, and S. Fan, "Fiber-optic Fabry–Perot acoustic sensor with multilayer graphene diaphragm," *IEEE Photon. Technol. Lett.*, vol. 10, no. 25, pp. 932–935, May 2013.
[24] G. D. VanWiggeren, T. K. Gaylord, D. D. Davis, M. I. Braiwish, E. N. Glytsis, and E. Anemogiannis, "Tuning, attenuating, and switching by controlled flexure of long-period fiber gratings," *Opt. Lett.*, vol. 26, no. 2, pp. 61–63, 2001.
[25] Y. Gong, T. Zhao, Y. Rao, and Y. Wu, "All-fiber curvature sensor based on multimode interference," *IEEE Photon. Technol. Lett.*, vol. 23, no. 11, pp. 679–681, Jun. 2011.